

The Global Hydrological Cycle and Atmospheric Shortwave Absorption in Climate Models under CO₂ Forcing

KEN TAKAHASHI

Atmospheric and Oceanic Sciences Program, Princeton University, Princeton, NJ.

ABSTRACT

The spread among the predictions by climate models for the strengthening of the global hydrological cycle (i.e. the global mean surface latent heat flux, LH, or, equivalently, precipitation) at a given level of CO₂-induced global warming is of the same magnitude as the inter-model mean. By comparing several climate models from the WCRP CMIP3 database under idealized CO₂ forcings, it is shown that differences in the increase in global atmospheric shortwave heating (SW_{abs}) induced by clear-sky absorption, presumably by water vapor, partly explains this spread. The increases in SW_{abs} and in LH present similar spreads across models but are anticorrelated, so the sum SW_{abs}+LH increases more robustly than either alone. This is consistent with a recently proposed theory (Takahashi, 2009) that predicts that this sum (or, equivalently, the net longwave divergence *minus the surface sensible heat flux*) is constrained by energy conservation and robust longwave physics.

The intermodel scatter in SW_{abs} changes is not explained by differences in the radiative transfer models or in intermodel differences in global water vapor content change but perhaps by more subtle aspects of the changes in the water vapor distribution. Nevertheless, the fact that the radiative transfer models generally underestimate the increase in SW_{abs} relative to the corresponding line-by-line calculation for a given change in water vapor content suggests that the climate models might be overestimating the rate of increase in the global hydrological cycle with global warming.

1. Introduction

Comprehensive climate models predict that the global hydrological cycle (or, equivalently, the global mean surface latent heat flux, LH, and precipitation) will increase at a significantly smaller [fractional] rate than atmospheric water vapor content with global warming (Mitchell et al., 1989; Allen and Ingram, 2002; Held and Soden, 2006). It has been argued that this smaller rate is set by energetic (i.e. radiative) considerations rather than by moist processes (Mitchell et al., 1989, Allen and Ingram, 2002). Climate models predict a rate of change in LH of around 2% per degree warming (Held and Soden, 2006). However, values from individual models can differ by a factor of five (e.g. Fig 2b in Held and Soden, 2006). Understanding what determines the mean change in LH and the scatter around it is important

for evaluating both climate models and observational estimates. In this study we address the inter-model differences from an analysis of available model results, and using an approach based on energy conservation, outlined next.

The global mean equilibrium energy budget for the atmosphere is

$$\text{LH} + \text{SH} + \text{SW}_{\text{abs}} = \text{LW}_{\text{div}} \quad (1)$$

where the terms, from left to right, represent surface latent and sensible heat fluxes, shortwave radiation absorbed by the atmosphere, and net atmospheric longwave flux divergence. This equation is expected to be approximately valid even if the ocean is not in equilibrium with an external radiative forcing, due to the relatively small heat capacity of the atmosphere. Under a perturbation in greenhouse gases, the change in the LW fluxes could be taken as a first approximation to consist in a radiative forcing (i.e. the direct effect of the perturbation in composition) and a response that

Corresponding author address:

Ken Takahashi, Instituto Geofísico del Perú, Calle Bada-joz 169, Lima 3, Peru. (e-mail: ken@chavin.igp.gob.pe)

scales with the temperature change (e.g. Allen and Ingram, 2002). The latter is physically justified to some extent by the temperature dependence of the Planck blackbody emission function and the observation that assuming fixed relative humidity, which implies that water vapor is mainly a function of temperature, provides a good approximation to the water vapor feedback in climate models (Soden and Held, 2006). An approximate model could be made for LH by using this LW model and ignoring changes in SH and SW_{abs} (Allen and Ingram, 2002), but there is no physical justification for doing the latter a priori. Furthermore, surface sensible heat *and* longwave radiative fluxes depend on the temperature difference between the surface and the surface air (δT), which is an additional degree of freedom that will not necessarily scale with global warming. An idealized physical model (Takahashi, 2008) suggests that the necessary additional constraint can be provided by considering the energy budget for the atmospheric layer above the cloud base level. In this idealized model, the change in SW_{abs}+LH is approximately determined by the changes in the longwave flux divergence in the layer above cloud base (LW_{div}^{acb}), which does not depend on the changes in δT and is, therefore, more robustly constrained by longwave physics.

The results from the present study indicate that the changes in SW_{abs}+LH (or, equivalently, LW_{abs}-SH) and, therefore, LW_{div}^{acb} (Takahashi, 2009) are robust functions of the changes in global temperature and in CO₂ concentrations across different models and experiments, but the rates of change in SW_{abs} alone are not, and this results in the scatter in the change in LH. A recent study by Lambert and Webb (2008, hereafter LW08) suggests that the net clear-sky radiative cooling is the robust process that constrains the increase in LH. The present study considers a larger set of climate models and determines that the change in radiative cooling does closely resemble the change in LH, but that the change in SW_{abs}+LH is more robust than either.

In the next section we describe the data used and the methodology, in section 3 we describe the results and their analysis and finally we present a discussion and main conclusions.

2. Data and methods

We analyze the output of eight climate models from the World Climate Research Programme (WCRP) Coupled Model Intercomparison Project 3 (CMIP3) database (Meehl et al., 2007; Table 1). Three experiments were considered in which CO₂ concentrations were increased and the other radiatively active species (except for water vapor) held fixed: one in which the climate models had an slab-ocean model and the CO₂ concentration

was instantly doubled (denoted 2xco2 in the WCRP CMIP3 database), and two others with full ocean general circulation models in which the CO₂ concentration was increased at a rate of 1% per year until doubling and quadrupling and then held constant (1pctto2x and 1pctto4x, respectively). Additionally, a twenty-year four-member ensemble run with GFDL CM2.1 under instantaneous doubling of CO₂ concentrations was considered (denoted 2xco2c).

The analysis was performed on the global and multi-year mean perturbations (indicated with Δ s) from the transient data in these experiments relative to the mean of the corresponding control runs. The data considered was surface air temperature perturbations (ΔT) and the perturbations in the terms in the atmospheric energy budget (1), computed from surface and top-of-the-atmosphere energy fluxes. It should be noted that although LW_{div}^{acb} is frequently mentioned in reference to the theory of Takahashi (2009), no calculation is explicitly made using fluxes at cloud base.

The analysis was made only for those periods during the runs in which the CO₂ concentrations are constant in time (i.e. for all time, after year 70, and after year 140 for the 2xco2/2xco2c, 1pctto2x and 1pctto4x runs, respectively). Since the radiative forcing of CO₂ is approximately linear on the logarithm of the concentrations, the forcing for the 1pctto4x run is twice as much as in the other two runs. We take advantage of this by dividing the perturbation data of the 1pctto4x run by a factor of two, which approximately yields the equivalent of a run in which the CO₂ concentration is increased by 0.5% per year until doubling, except for possible non-linear effects that might arise from the larger forcing (Hansen et al., 2005).

To reduce the impact of high-frequency unforced internal climate variability in the analysis, the data were subjected to time averaging before the analysis. Thirty and twenty-year means were considered for the 1pctto2x and 1pctto4x runs, respectively, while, for the 2xco2 the means were annual for years 1-5, biennial for years 6-10, pentadal for years 11-20, and lastly for the rest of the run. The latter averaging was done to yield approximately uniform spacing in global surface air temperature perturbations (ΔT), considering that the slab models equilibrate within twenty years.

A linear relationship was assumed between ΔT and the perturbation in a generic energy budget term X :

$$\Delta X \approx (\partial X / \partial T) \Delta T + F_X \quad (2)$$

and the coefficients $\partial X / \partial T$ and F_X were determined by least-square regression and 95% confidence intervals for the fit are given. The slope parameter $\partial X / \partial T$ is a measure of the response of the climate system mediated

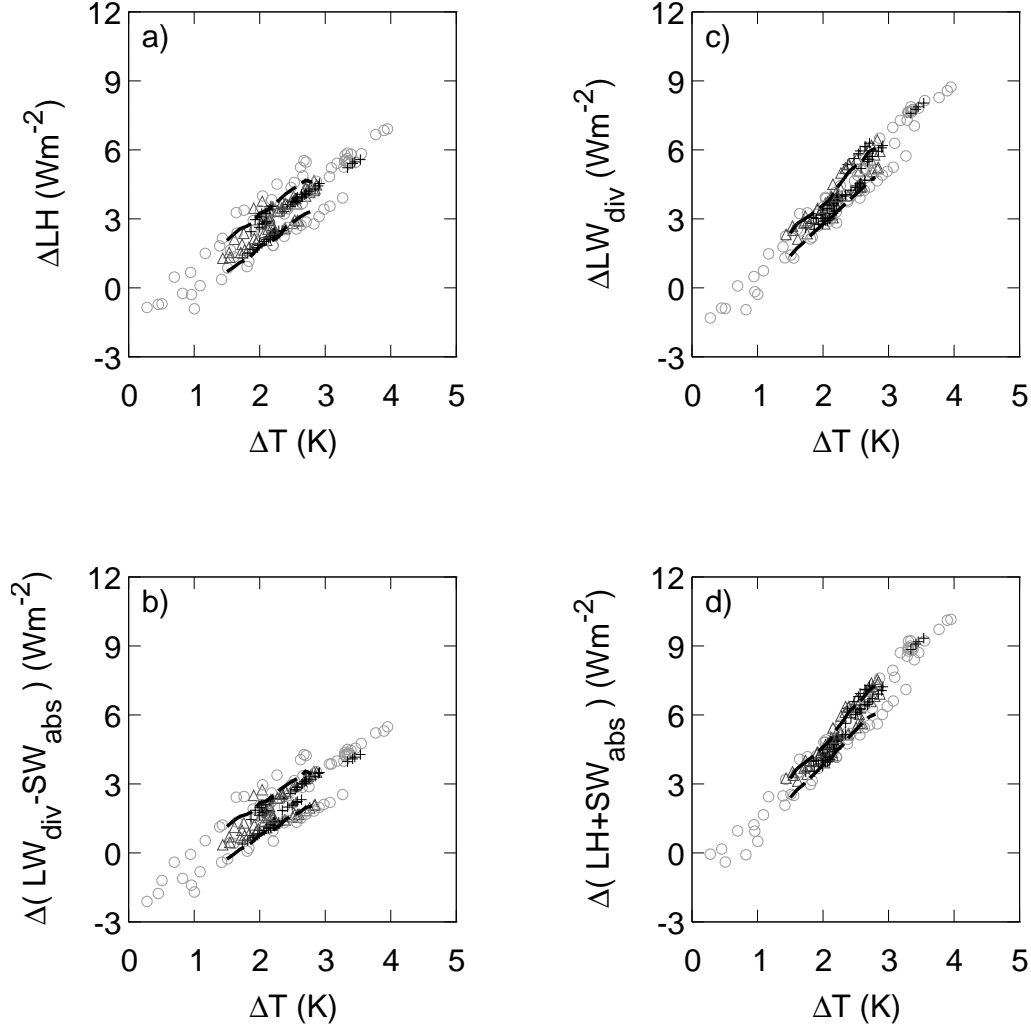


FIG. 1. Changes in global mean a) surface latent heat flux (ΔLH), b) net radiative cooling ($\Delta[LW_{\text{div}} - SW_{\text{abs}}]$), c) longwave radiative cooling (ΔLW_{div}), and d) surface latent heat flux plus shortwave heating ($\Delta[LH + SW_{\text{abs}}]$), as a function of global warming (ΔT) for all models and the 2xc02, 1pctto2x and 1pctto4x runs (\circ , Δ and $+$, respectively). The thick dashed lines indicate the multimodel/multirun mean (binned by ΔT) plus and minus the corresponding standard deviation.

by ΔT , while the intercept F_X represents a direct forcing by the change in the CO₂ concentrations (i.e. not directly related to ΔT). This approach was initially proposed by Gregory et al. (2004) in the context of climate sensitivity and forcing and has also been recently used in the context of the global hydrological cycle by LW08.

Under the assumption that there is a “true” linear process (2) that underlies *all* of the climate models, so that the data from each of the latter results from this single process plus random model-dependent effects, then the slope and intercept coefficients estimated for each of the climate models and the corresponding er-

ror estimates can be optimally combined¹ to estimate of the parameters A of the linear process according to:

$$\hat{A} = \hat{\sigma}_A^2 \sum_i \frac{A_i}{\sigma_{A_i}^2} \quad (3)$$

where A_i is the coefficient estimated for the climate model i with estimated error σ_{A_i} and \hat{A} is the multimodel optimal estimate. The estimated error for (3) is given by:

$$\hat{\sigma}_A = \left(\sum_i \sigma_{A_i}^{-2} \right)^{-1/2}. \quad (4)$$

¹By minimizing the cost function $\sum_i (A_i - \hat{A})^2 / \sigma_i^2$.

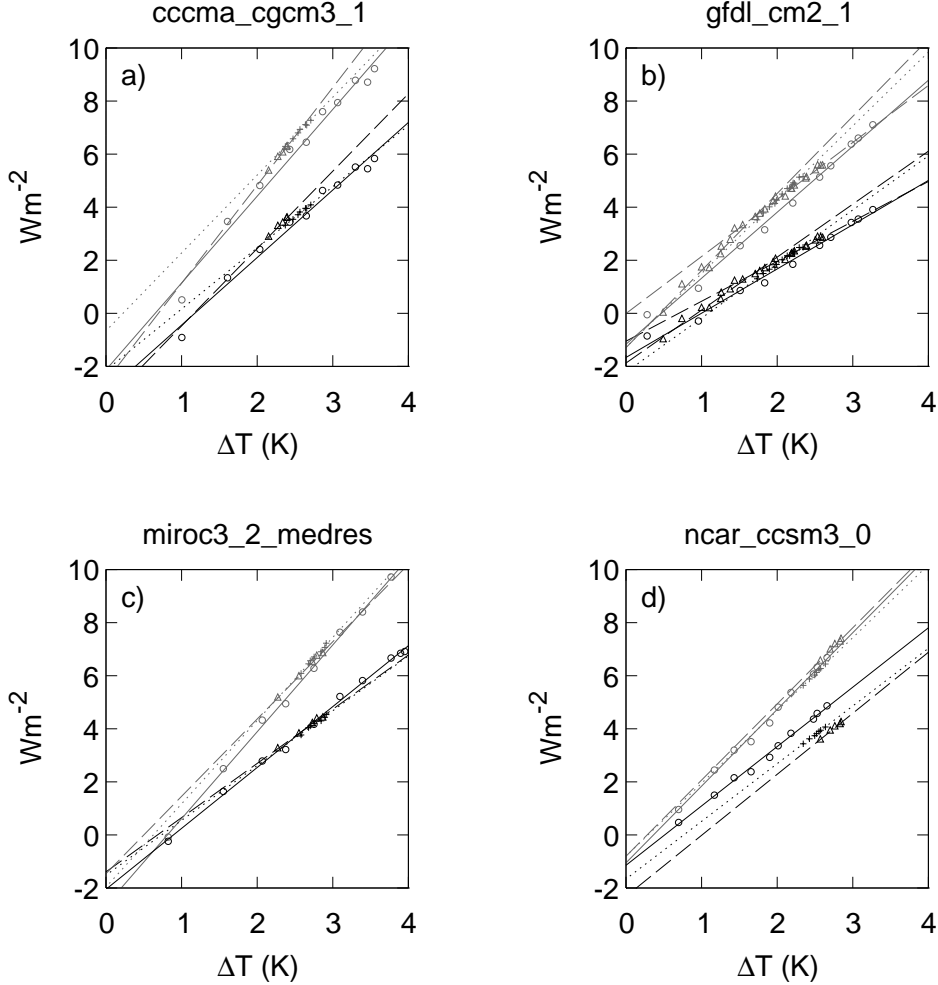


FIG. 2. Changes in global mean surface latent heat flux (ΔLH ; black), and surface latent heat flux plus shortwave heating ($\Delta[LH+SW_{abs}]$; gray), as a function of global warming (ΔT) for four selected models and the $2\times CO_2$, $1pctto2x$ and $1pctto4x$ runs (\circ , \triangle and $+$, respectively). The linear fits (Table 1) for each run are indicated by solid, dashed and dotted lines, respectively. For the *gfdl_cm2_1* model, the four-member ensemble mean of a 20-year fully coupled run with instantly doubled CO₂ concentrations are indicated with \triangle as well (for $\Delta T \leq 1.5K$).

Also, a multi-model multi-run ensemble dataset was set up for the energy budget terms by linearly interpolating the individual data onto common values of ΔT . The mean and standard deviation were calculated for those values of ΔT for which at least 7 models/runs had data and the linear model (2) was also fit to the mean.

Additional data from a standard case run with stand-alone versions of the radiative transfer schemes used in the CMIP3 models considered from the Radiative Transfer Model Intercomparison Project (RTMIP; Collins et al., 2006a), were also compared to the climate model data.

3. Results and analysis

In Fig. 1a we show ΔLH plotted against the change in global mean surface air temperature (ΔT) for all climate models and runs. The linear model (2) with a single set of coefficients is a reasonable representation of the overall behavior of the climate models, although significant scatter exists across them. The standard deviation with respect to the multi-model/run ensemble mean equals 0.71 Wm^{-2} in this case. The estimated slope and forcing coefficients for this ensemble mean are $2.1 \text{ Wm}^{-2}/K$ and -1.8 Wm^{-2} , respectively, which is consistent with the results of LW08. These values are also consistent with the corresponding optimal combination of the estimates for each model and run (Table 1), although the scatter across models is significant

Id	Climate model (WCRP CMI3 Id)	Run	$\partial\text{LH}/\partial T$ (Wm ⁻² /K)	F_{LH} (Wm ⁻²)	$\partial(\text{LH}+\text{SW}_{\text{abs}})/\partial T$ (Wm ⁻² /K)	$F_{\text{LH}+\text{SW}_{\text{abs}}}$ (Wm ⁻²)	$\partial\text{LW}_{\text{div}}/\partial T$ (Wm ⁻² /K)	$F_{\text{LW}_{\text{div}}}$ (Wm ⁻²)
1	CCCma CGCM 3.1 (cccma_cgcm3.1)	2xco2	2.55±0.27	-2.99±0.74	3.27±0.35	-2.13±0.96	3.18±0.32	-2.85±0.86
		1pctto2x	2.92±0.44	-3.39±1.01	3.69±0.50	-2.56±1.16	3.54±0.43	-3.16±0.99
		1pctto4x	2.31±0.25	-2.14±0.63	2.94±0.35	-0.66±0.89	2.83±0.27	-1.36±0.68
2	GFDL CM2.0 (gfdl_cm2.0)	2xco2	1.63±0.21	-1.69±0.46	2.44±0.22	-1.11±0.48	2.37±0.12	-1.95±0.27
		1pctto2x	1.64±0.23	-1.05±0.45	2.35±0.32	-0.16±0.63	2.03±0.27	-0.50±0.54
		1pctto4x	2.04±0.36	-2.13±0.77	2.81±0.47	-1.26±1.01	2.46±0.28	-1.52±0.60
3	GFDL CM2.1 (gfdl_cm2.1)	2xco2	1.67±0.15	-1.66±0.35	2.49±0.18	-1.16±0.41	2.42±0.13	-2.25±0.31
		2xco2c	2.00±0.44	-1.87±0.48	2.91±0.59	-1.29±0.63	2.72±0.49	-1.82±0.53
		1pctto2x	1.50±0.09	-1.05±0.20	2.15±0.10	-0.01±0.22	1.80±0.05	-0.34±0.11
		1pctto4x	2.04±0.13	-2.22±0.26	2.78±0.14	-1.28±0.29	2.41±0.07	-1.57±0.14
4	GISS E-R (giss_model_e_r)	2xco2	2.79±0.29	-1.86±0.58	3.18±0.30	-1.73±0.60	2.85±0.30	-2.06±0.60
		1pctto2x	2.29±NA	-0.99±NA	2.71±NA	-0.90±NA	2.32±NA	-1.11±NA
		1pctto4x	2.22±0.59	-1.33±1.22	2.56±0.66	-1.09±1.38	2.21±0.49	-1.52±1.02
5	INM CM 3.0 (inmcm3.0)	2xco2	3.13±0.90	-3.45±1.88	3.57±1.09	-3.15±2.30	2.82±1.77	-2.75±3.71
		1pctto2x	1.82±0.48	-0.91±0.93	2.18±0.59	-0.49±1.15	1.85±0.53	-0.97±1.03
		1pctto4x	1.74±0.37	-0.81±0.75	2.17±0.35	-0.53±0.72	1.99±0.26	-1.17±0.52
6	MIROC 3.2 (medres) (miroc3.2.medres)	2xco2	2.29±0.09	-2.05±0.27	3.27±0.10	-2.66±0.29	3.10±0.08	-3.48±0.25
		1pctto2x	2.04±0.36	-1.39±0.95	2.91±0.38	-1.46±1.01	2.80±0.19	-2.14±0.52
		1pctto4x	2.07±0.41	-1.52±1.15	3.14±0.47	-1.96±1.29	2.87±0.23	-2.21±0.63
7	MPI-ECHAM5 (mpi_echam5)	1pctto2x	2.01±0.44	-1.10±1.16	2.56±0.51	0.23±1.34	2.51±0.18	-0.76±0.48
		1pctto4x	1.80±1.03	-0.77±3.53	2.50±1.11	0.52±3.80	2.28±0.52	-0.03±1.80
8	NCAR CCSM 3.0 (ncar_ccsm3.0)	2xco2	2.24±0.13	-1.14±0.26	2.89±0.16	-1.05±0.32	2.55±0.15	-1.58±0.29
		1pctto2x	2.30±0.48	-2.31±1.32	2.87±0.66	-0.80±1.80	2.52±0.38	-2.02±1.04
		1pctto4x	2.17±0.15	-1.66±0.37	2.74±0.17	-0.80±0.43	2.19±0.17	-1.08±0.43
	Standard deviation	2xco2	0.55	0.81	0.43	0.83	0.32	0.64
	of fit parameters	1pctto2x	0.45	0.88	0.50	0.90	0.57	0.97
	across models	1pctto4x	0.20	0.58	0.29	0.72	0.31	0.62
		All runs	0.42	0.78	0.42	0.92	0.43	0.89
	Multimodel optimal	2xco2	2.17±0.06	-1.69±0.15	3.00±0.07	-1.70±0.17	2.76±0.06	-2.39±0.13
	estimate	1pctto2x	1.64±0.08	-1.15±0.17	2.28±0.09	-0.17±0.19	1.94±0.05	-0.48±0.10
		1pctto4x	2.10±0.08	-1.94±0.18	2.75±0.09	-1.07±0.21	2.41±0.05	-1.52±0.12
		All runs	2.00±0.04	-1.59±0.10	2.74±0.05	-1.05±0.11	2.32±0.03	-1.29±0.07
	Multi-model/run ensemble mean		2.10±0.10	-1.77±0.23	3.04±0.11	-1.77±0.25	2.78±0.10	-2.30±0.23

TABLE 1. Estimated linear fit parameters with 95% standard errors of ΔLH , $\Delta(\text{LH}+\text{SW}_{\text{abs}})$ and $\Delta\text{LW}_{\text{div}}$ against ΔT for the different WCRP CMIP3 models and runs considered and multimodel estimates, excluding the GFDL CM2.1 2xco2c run (see text for details).

(standard deviations of 0.4 Wm⁻²/K and 0.8 Wm⁻², respectively).

The net radiative cooling ($\Delta[\text{LW}_{\text{div}}-\text{SW}_{\text{abs}}]$; Fig 1b, Table 1) has a similar behavior to ΔLH , indicative of the relatively small magnitude of ΔSH (not shown), so their scatter across models and runs are also similar. On the other hand, the longwave cooling ($\Delta\text{LW}_{\text{div}}$; Fig 1c) is more robust than either (standard deviation with respect to the multi-model/run ensemble mean is 75% of the value for ΔLH). This indicates that the shortwave heating is a source of scatter rather than a robust feature across models. Indeed, as predicted by theory (Takahashi, 2009), the quantity $\Delta[\text{LH}+\text{SW}_{\text{abs}}]$ (Fig 1d) shows an even smaller scatter (68% of that of ΔLH), which indicates that the scatter in ΔLH and in $\Delta\text{SW}_{\text{abs}}$ are anticorrelated.

The differences in scatter indicated above and visually evident in Fig. 1 are not reflected in the linear fit coefficients estimated for the various climate models/runs (Table 1). A reason for this is illustrated in Fig. 2, in which ΔLH and $\Delta[\text{LH}+\text{SW}_{\text{abs}}]$ for the different runs are plotted against ΔT for four representative climate models. Although in general the data from different runs tend to cluster around the same lines for

each model, the linear fits for each run can have significantly different coefficients. An interesting exception is the ncar_ccsm3.0 model (Fig. 1d), for which the ΔLH in the three runs can be clearly seen to lie on well separated approximately parallel lines, whereas the $\Delta[\text{LH}+\text{SW}_{\text{abs}}]$ data lies on the same line. This is clear evidence that $\Delta[\text{LH}+\text{SW}_{\text{abs}}]$ is better constrained by the longwave physics than ΔLH alone in this model.

The gfdl_cm2.1 data (Fig. 2b) is particularly illuminating for understanding the different fit parameters between runs, as it also includes the 2xco2c data, corresponding to the ensemble mean of the full-model twenty-year run in which the CO₂ concentration is instantly doubled (same as the 2xco2 run except that the model has full ocean dynamics, as in 1pctto2x). The linear fits for both ΔLH and $\Delta(\text{LH}+\text{SW}_{\text{abs}})$ are rather well constrained from the data for each of the runs, but the corresponding lines are well differentiated (Fig. 2b, Table 1). During the early period when ΔT is small, the 2xco2c data starts close to the slab model 2xco2 run but, as ΔT increases, it diverges towards the 1pctto2x results, along which the climate then converges back towards the 2xco2 run at higher values of ΔT . This nonlinear behavior has been previ-

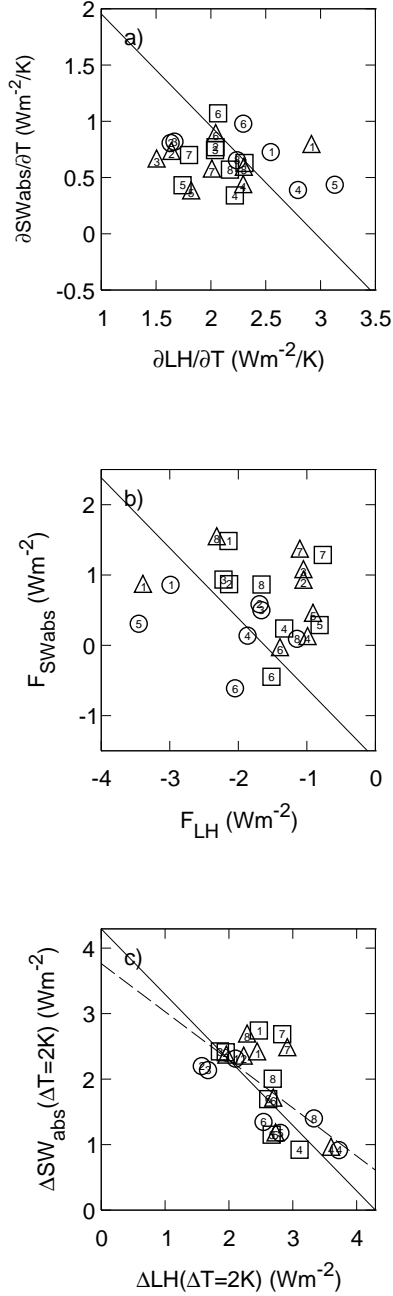


FIG. 3. a) Slope and b) intercept parameters for the linear regression with ΔT of ΔLH and ΔSW_{abs} plotted against each other. c) Estimates for ΔLH and ΔSW_{abs} at $\Delta T = 2\text{K}$ using the linear regression fits (Table 1). Models are identified by the numbers in Table 1. The $2x_{\text{co}2}$, $1\text{pctto}2x$ and $1\text{pctto}4x$ runs are indicated with \circ , \triangle and \square , respectively. The solid lines represent the case in which the two variables plotted add up to the value corresponding to the linear fit to the multimodel/multirun ensemble mean $\Delta(LH+SW_{\text{abs}})$. The dashed line in c) is the linear fit between the variables plotted.

ously observed in the radiative fluxes at the top of the atmosphere (Forster and Taylor, 2006; Williams et al., 2008; Winton et al., 2009) and is particularly strong in the GFDL models (Forster and Taylor, 2006; Winton et al., 2009). In those studies, the nonlinearity is found to emerge from the action of another degree of freedom in addition to ΔT associated with the way the ocean heat uptake in the full climate model affects the warming and cloud distribution (Williams et al., 2008; Winton et al., 2009). To the extent that this effect is small, the full-model climate trajectories will stay close to those of the slab model, but the fit of a linear model to a limited portion of the full model runs could lead to misleading results. Consistent with this interpretation, the results of the optimal combination of the fit coefficients obtained for the $2x_{\text{co}2}$ run (with no ocean dynamics) are similar to the ones that correspond to the multi-model/run ensemble (Table 1), even though the larger range in ΔT in the former was not included and, therefore, can not dominate the fit in the latter. Therefore, we believe that the optimal combination of the $2x_{\text{co}2}$ runs and the multi-model/run ensemble will provide a more reliable depiction of the robust behavior common to all models and runs, which does not include the non-linearities that are apparently associated with dynamical aspects of ocean adjustment.

As previously mentioned, the smaller scatter in $\Delta[LH + SW_{\text{abs}}]$ compared to ΔLH for given values of ΔT implies an anticorrelation between ΔLH and ΔSW_{abs} . This can be seen in Fig. 3c, in which the linear fits (Table 1) have been used to estimate the values of ΔLH and ΔSW_{abs} at the value $\Delta T = 2\text{K}$, which is approximately the value for which there is the most nearby data and, therefore, the errors associated with extrapolation would be least severe. In this figure, we show that there is indeed an anticorrelation between the two quantities (linear correlation coefficient of -0.66) and the fitted linear relation is close to the expected one. On the other hand, very little correlation is found if the analysis is done with the linear fit coefficients themselves (Fig. 3a and b), as expected from the previous discussion of the errors that can be made with limited data.

The forcing components for LH and for $[LH+SW_{\text{abs}}]$ are indistinguishable in the multi-model/run ensemble (Table 1), consistent with SW_{abs} being directly controlled by water vapor (hence, by temperature and not by CO₂ concentrations) through the physics of radiative transfer. As a result of this, after the CO₂ concentration is changed but before any warming takes place, ΔLH alone has to balance the associated forcing. Although the doubling of CO₂ does have an effect on SW_{abs} , it is about an order of magnitude smaller than the effect of the associated change in water vapor (Collins et al., 2006)

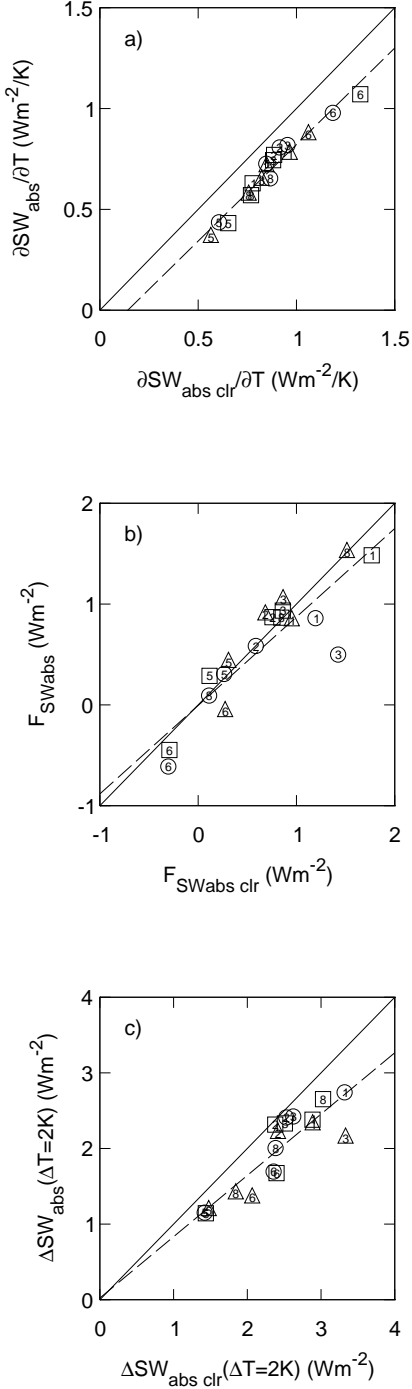


FIG. 4. Similar to Fig. 3 but the solid lines are 1:1 lines included as reference.

On the other hand, the effect of clouds on ΔSW_{abs} can not be dismissed *a priori*. However, the scatter in ΔSW_{abs} is well explained by the clear-sky component (Fig. 4), indicating that clouds are not an important source of scatter. There is also no significant relation between ΔSW_{abs} and the clear-sky upward shortwave

flux at the surface (not shown), which indicates that surface albedo changes are also unimportant. This suggests that the scatter in ΔSW_{abs} is controlled by water vapor but, while ΔSW_{abs} can differ by a factor of 3 across models, the changes in global mean water vapor content are robust (Held and Soden, 2006) and the associated scatter cannot explain the differences in ΔSW_{abs} .

Another possible source for the scatter in ΔSW_{abs} is differences among radiative transfer codes, as found in the RTMIP project, in which stand-alone versions of various of these codes subjected to exactly the same change in water vapor (a uniform 20% increase for an idealized profile) resulted in different values of ΔSW_{abs} (Collins et al., 2006a). However, the `ncar_ccsm3.0` model spans the full range of the scatter in ΔSW_{abs} (Fig. 4c) despite having the same radiative transfer code in all runs. Furthermore, the scatter in the RTMIP ΔSW_{abs} data mentioned above is not correlated with the scatter in the corresponding WCRP CMIP3 data (present study; not shown).

The previous analysis suggests that the scatter in ΔSW_{abs} across models and runs is perhaps associated with subtler aspects of the water vapor changes, particularly on the details of the spatial distribution of the changes in moisture in the models. For instance, in the GFDL CM2.1 model, the changes in shortwave absorption are concentrated in the tropics above the 500 hPa level (not shown), which suggests that small absolute changes in upper-troposphere moisture content have a significant effect on SW_{abs} . This is something that could be tested with the radiative kernel approach (Held and Soden, 2000; Soden et al., 2008).

An aspect in Fig. 4 that is worth commenting is that although both of the linear fit coefficients for the full sky and clear sky SW_{abs} are well correlated (reflecting a direct physical link), the slope coefficient for the clear sky is systematically higher than for the full sky by around $0.1 \text{ Wm}^{-2}/\text{K}$ (Fig. 4a), which results in smaller values in ΔSW_{abs} at $\Delta T = 2\text{K}$ for full sky relative to clear sky by about 20% (Fig. 4c). This is unlikely to be related to changes in clouds with warming, as this is not a robust feature across models (e.g. Bony and Dufresne, 2005), but might be related to the basic-state reflection of incoming shortwave radiation by high clouds, which reduces both the basic-state absorption and the increase in this absorption for a given change in water vapor. On the other hand, this would be expected to result a proportional reduction rather than the uniform one seen in Fig. 4a, so this is probably not the full explanation.

4. Discussion and conclusions

The results of this study support the theoretical prediction that the change in the sum of the surface la-

tent heat flux and atmospheric shortwave absorption (or, equivalently, the net longwave divergence minus the surface sensible heat flux) should vary with CO₂-induced global warming more robustly than any other combination of the terms in the energy budget of the atmosphere, as these combinations are proxies for the longwave flux divergence above cloud base, which is determined by longwave physics more robustly than the total atmosphere longwave flux divergence (Takahashi, 2009). The results of this study indicate that $\Delta[\text{LH} + \text{SW}_{\text{abs}}]$ varies at a rate of around 2-4 Wm⁻²/K with ΔT and that doubling CO₂ has a direct effect (i.e. “forcing”) of around -1.8 Wm⁻².

Despite the fact that clear-sky water vapor changes appear to determine the changes in $\Delta\text{SW}_{\text{abs}}$, the understanding of what are the important aspects of the former is low. It is only recently that climate models are converging towards producing realistic (sufficiently strong) tropospheric clear-sky shortwave absorption (Wild et al., 2006). Although the physics behind this absorption are well understood from first principles, subtle deficiencies in the depiction of the spectroscopic properties of water vapor have substantial consequences for the clear-sky absorption of shortwave radiation (e.g. Collins et al., 2006b). Furthermore, the convergence in present-day absorption does not necessarily translate to the climate change case and, as shown by Collins et al. (2006a), there is relatively large inter-model discrepancies in the changes in clear-sky surface shortwave flux associated with water vapor that could lead to a systematic error in all models. Specifically, the increase in SW_{abs} associated with an idealized change in water vapor is underestimated by almost all climate models relative to the corresponding line-by-line calculation, which implies that the models are potentially *overestimating* the increase in LH associated with global warming. On the other hand, the physics relevant to the results of the present study are apparently not those of the interaction between the shortwave radiation and water vapor, but rather the processes that control the spatial aspects of the changes in water vapor that lead to differences in the global mean absorption of shortwave radiation by the atmosphere, which are even less well understood.

Considering that $\Delta[\text{LH} + \text{SW}_{\text{abs}}]$ varies with ΔT at a rate of 2-4 Wm⁻²/K and, since water vapor increases with global warming (e.g. Held and Soden, 2000), it is unlikely that SW_{abs} would decrease with increasing T . Thus, the upper bound for the increase in LH per degree global warming in the climate models would be around 4 Wm⁻²/K or 5%/K, which is lower than the Clausius-Clapeyron scaling (around 7%/K) that is followed by the total water vapor content. For LH to increase following the Clausius-Clapeyron scaling (e.g. Wentz et al., 2007), climate models would need to pro-

duce a $\partial[\text{LH} + \text{SW}_{\text{abs}}]/\partial T$ about 100% higher than they currently do, assuming that $\partial\text{SW}_{\text{abs}}/\partial T$ is represented correctly. This seems unlikely to occur in future models in the light of the theory of Takahashi (2009), according to which $\text{LH} + \text{SW}_{\text{abs}}$ is a proxy for the longwave flux divergence above cloud base, which depends on relatively well established longwave physics. It is possible, however, that cloud longwave effects could be systematically underestimated by the models. Perhaps a way in which such effects could lead to an enhanced $\partial[\text{LH} + \text{SW}_{\text{abs}}]/\partial T$ is by having low clouds strongly increase with ΔT (opposite to what most models predict; Bony and Dufresne, 2005), so that the longwave emission towards the surface is enhanced. However, this would also lead to an opposing enhancement of the absorption of the radiation from the surface, so it seems unlikely that the *net* flux at cloud base could be sufficiently increased by this process.

It is interesting to consider the implications of having $\Delta\text{SW}_{\text{abs}}$ relatively unconstrained by the present state of knowledge, with the exception that we expect it to increase with increasing ΔT . In particular, this means that ΔLH does not even have to be positive. For instance, we can make an extreme thought experiment in which instead of shortwave absorption by water vapor being dominated by a few almost-saturated bands in the near-infrared, we have it associated with unsaturated weaker and wider bands, but resulting in the same present-day absorption. Then we could expect this absorption to change proportionally to water vapor and, therefore, to increase according to the Clausius-Clapeyron relation. Taking a mid-tropospheric value of 10%/K for this relation and a present-day shortwave absorption of 70 Wm⁻²/K (Kiehl and Trenberth, 1997), then the increase would be at a rate of around 7 Wm⁻²/K. Thus, subtracting this from the ensemble value of 3 Wm⁻²/K, which is attributable to longwave physics, would imply that latent heat flux would have to *decrease* by around 4 Wm⁻²/K as the climate warms. Although this is a hypothetical scenario that does not agree with the present understanding of the physics of shortwave absorption, it highlights the need of further study into the issue if the changes in the global hydrological cycle are to be quantitatively understood.

Acknowledgments. The author thanks I. M. Held for useful discussions and comments on the manuscript and G. A. Vecchi for useful discussions, as well as W. D. Collins and V. Ramaswamy for providing the RT-MIP data. The comments from two anonymous reviewers helped improve the manuscript. The CMIP3 model data were made available by the Program for Climate Model Diagnosis and Intercomparison at the U.S. Department of Energy’s Lawrence Livermore Na-

tional Laboratory. This research was supported by the National Oceanic and Atmospheric Administration (NOAA) Climate and Global Change Postdoctoral Fellowship Program, administered by the University Corporation for Atmospheric Research, under award NA06OAR4310119 from the NOAA Climate Programs Office, U.S. Department of Commerce. The statements, findings, conclusions, and recommendations are those of the author and do not necessarily reflect the views of NOAA or the U.S. Department of Commerce.

REFERENCES

- Allen, M. R., and Ingram, W. J., 2002: Constraints on future changes in climate and the hydrologic cycle. *Nature* 419, 224-232
- Bony, S., and Dufresne, J.-L., 2005: Marine boundary layer clouds at the heart of tropical cloud feedback uncertainties in climate models. *Geophys. Res. Lett.* 32, L20806.
- Collins, W. D., and Coauthors, 2006a: Radiative forcing by well-mixed greenhouse gases: Estimates from climate models in the Intergovernmental Panel on Climate Change (IPCC) Fourth Assessment Report (AR4). *J. Geophys. Res.* 111, D14317.
- Collins, W. D., Lee-Taylor, J. M., Edwards, D. P., and Francis, G. L., 2006b: Effects of increased near-infrared absorption by water vapor on the climate system. *J. Geophys. Res.* 111, D18109.
- Forster, P. M. F. and Taylor, K. E., 2006: Climate forcings and climate sensitivities diagnosed from coupled climate model integrations. *J. Climate* 19, 6181-6194.
- Gregory, J. M., Ingram, W. J., Palmer, M. A., Jones, G. S., Stott, P. A., Thorpe, R. B., Lowe, J. A., Johns, T. C., and Williams, K. D., 2004: A new method for diagnosing radiative forcing and climate sensitivity. *Geophys. Res. Lett.* 31, L03205.
- Hansen, J. and coauthors, 2005: Efficacy of climate forcings. *J. Geophys. Res.* 110, D18104.
- Held, I. M. and Soden, B. J., 2000: Water vapor feedback and global warming. *Annu. Rev. Energy Environ.* 25, 441-475.
- Held, I. M. and Soden, B. J., 2006: Robust responses of the hydrological cycle to global warming. *J. Climate* 19, 5686-5699.
- Kiehl, J. T., Hack, J. J., Bonan, G. B., Boville, B. A., Briegleb, B. P., Williamson, D. L., and Rasch, P. J., 1996: Description of the NCAR Community Climate Model (CCM3). NCAR Technical Note 420.
- Kiehl and Trenberth, 1997: Earth's annual global mean energy budget. *Bull. Amer. Met. Soc.* 78, 197-208.
- Lambert, F. H., and Webb, M. J., 2008: Dependency of global mean precipitation on surface temperature. *Geophys. Res. Lett.* 35, L16706.
- Meehl, G. A., Covey, C., Delworth, T., Latif, M., McAvaney, B., Mitchell, J. F. B., Stouffer, R. J., and Taylor, K. E., 2007: The WCRP CMIP3 multimodel dataset: A new era in climate change research. *Bull. Amer. Met. Soc.* 1383-1394
- Mitchell, J. F. B., Wilson, C. A., and Cunningham, W. M., 1989: On CO₂ climate sensitivity and model dependence of results. *Q. J. Roy. Met. Soc.* 113, 293-3322.
- Soden, B. J. and Held, I. M., 2006: An assessment of climate feedbacks in coupled ocean-atmosphere models. *J. Climate* 19, 3354-3360
- Soden, B. J., Held, I. M., Colman, R., Shell, K. M., Kiehl, J. T., and Shields, C. A., 2008: Quantifying climate feedbacks using radiative kernels. *J. Climate* 21, 14, 3504-3520.
- Takahashi, K., 2009: Radiative constraints on the hydrological cycle in an idealized radiative-convective equilibrium model. *J. Atmos. Sci.* 66, 77-91.
- Wentz, F. J., Ricciardulli, L., Hilburn, K., and Mears, C., 2007: How much more rain will global warming bring? *Science* 317, 233-235.
- Wild, M., Long, C. N., and Ohmura, A., 2006: Evaluation of clear-sky solar fluxes in GCMs participating in AMIP and IPCC-AR4 from a surface perspective. *J. Geophys. Res.* 111, D01104.
- Williams, K. D., Ingram, W. J., and Gregory, J. M., 2008: Time variation of effective climate sensitivity in GCMs. *J. Climate* 21, 5076-5090.
- Winton, M., Takahashi, K., and Held, I. M., 2009: Importance of ocean heat uptake efficacy to transient climate change. Submitted to *J. Climate*.

Printed May 19, 2009.